Empa
Überlandstrasse 129
CH-8600 Dübendorf
T +41 58 765 11 11
www.empa.ch

Empa
Materials Science and Technology

Comparison of CNOSSOS-EU (Air) & FLULA2

Imprint

Commissioned by the Swiss Federal Office for the Environment (FOEN), Noise and NIR Division, CH-3003 Bern

The FOEN is an agency of the Federal Department of the Environment, Transport, Energy and Communications (DETEC).

Contractor:	Empa – Swiss Federal Laboratories for Materials Science and Technology
	Laboratory for Acoustics / Noise Control
Authors:	Stefan Schalcher Jonas Meister Beat Schäffer

Number of pages:	23
Mandate No.:	5214.027361
Empa Report No.:	5214.027361-2

Dübendorf, 26 January 2022

Project leader:

Dr. Beat Schäffer

Laboratory for Acoustics & Noise Control

Laboratory head:

Dr. Jean-Marc Wunderli

Note: This report and associated data are archived for 10 years.

This report was prepared under contract to the Federal Office for the Environment (FOEN). The contractor bears sole responsibility for the content.

Content

Abstract

CNOSSOS-EU describes the aircraft noise calculation method to be used in Europe and proposes default values for the calculations. It further states that the input data should reflect the actual usage and that in general there should be no reliance on default input values. The current Swiss aircraft noise calculation model FLULA2 consists of a different calculation method and a corresponding sound source database derived from measurement campaigns in Switzerland. While both, FLULA2 and CNOSSOS-EU, are best-practice models, their modelling approaches are inherently different. In this report, the two models are compared formally and based on noise exposure calculations and corresponding measurements of several thousand single flight events around Zurich and Geneva airports in Switzerland, to test whether FLULA2 conforms with CNOSSOS-EU. For the CNOSSOS-EU calculations, the CNOSSOS-EU equivalent program AEDT was used.

Results show that while FLULA2 and CNOSSOS-EU use disparate modelling approaches and emission model descriptions, these differences only moderately affect the calculation results. Both FLULA2 and CNOSSOS-EU reproduced the sound exposure (single event level) L_{AE} well. For FLULA2, a mean difference of +0.1 dB with a standard deviation of 2.2 dB between calculations and measurements was found, while CNOSSOS-EU calculations with default input data yielded a mean difference of –0.4 dB with a standard deviation of 2.5 dB. Further, results of the two models agree well, with a mean difference of +0.5 dB (FLULA2 minus CNOSSOS-EU) and a standard deviation of 2.3 dB. Finally, exemplary calculations for two narrow-body aircraft types around Zurich airport showed that the agreement between the models may even be improved if the input data for CNOSSOS-EU (NPD data, flight profiles) are adjusted to local conditions.

Thus, FLULA2 yields similar results as CNOSSOS-EU, with differences on average below 1 dB, and there are no systematic differences between the modelling results. This leads to the conclusion that, despite different modelling approaches, FLULA2 is equivalent to CNOSSOS-EU on the airport scale, i.e., when used to calculate averaged noise exposures of complex scenarios such as yearly air traffic.

1. Mandate

By contract from May 25, 2021, the Laboratory for Acoustics / Noise Control at Empa, the Swiss Federal Laboratories for Materials Science and Technology, was mandated by the Swiss Federal Office for the Environment FOEN to conduct a study on road traffic and aircraft noise modelling (Empa project No. 5214.027361). This involved comparisons of the models regarding model structure and calculation results of relevant exposure cases. The results are documented in separate reports, namely, the comparison of (i) the Swiss sonROAD18 and CNOSSOS-EU road traffic noise emission models in Empa report No. 5214.027361-1, (ii) the Swiss FLULA2 and CNOSSOS-EU aircraft noise engineering models in Empa report No. 5214.027361-2, and (iii) the Swiss sonAIR and CNOSSOS-EU aircraft noise engineering models in Empa report No. 5214.027361-3.

In Switzerland, FLULA2 is one of three programs currently recommended by the Federal Office for the Environment FOEN as a tool for official aircraft noise calculations. As the next-generation aircraft noise program sonAIR is currently in the phase of being approved for official calculations in Switzerland and thus replacing FLULA2 in the near future, both aircraft noise models were compared in this study. These comparisons were made with the goal to assess the conformity of sonROAD18, FLULA2 and sonAIR with CNOSSOS-EU. They are the follow-up of the comparison of railway noise models [7].

The **present report No. 5214.027361-2** documents the comparison of the aircraft noise models **FLULA2 and CNOSSOS-EU**.

2. Introduction

The Environmental Noise Directive (END) of 2002 [9] specifies that the EU member states must prepare and submit noise exposure maps every five years. Its original Annex II about the assessment methods describes the adaptation of national computation methods.

In 2015, the EU published the CNOSSOS-EU model in the Commission Directive (EU) 2015/996 [10] as a replacement of the original Annex II of the END [9], which, among other noise sources, describes the aircraft noise model. A corrigendum to the Commission Directive (EU) 2015/996 was published in 2018 [11], and an amendment for adaptation to scientific and technical progress in 2020 in the Commission Delegated Directive (EU) 2021/1226 [12]. These model prescriptions are referred to as "CNOSSOS" in the following account. CNOSSOS describes the aircraft noise calculation method [10-12] and proposes default values for the calculations (aerodynamic coefficients, aircraft types, procedural step profiles, fixed point profiles, aircraft weights, jet engine coefficients, and noise-power-distance relationships (NPD data) [10]. However, [10] states that in the application of the method, the input data should reflect the actual usage, and that in general there should be no reliance on default input values.

In Switzerland, the model FLULA2 [6] developed at Empa is one of three aircraft noise models used for official aircraft noise calculations [1]. This model consists of a specific calculation method (time-step approach) and corresponding sound source database [6], which is also publicly available and used for official calculations [2].

The present report documents the results of a systematic comparison of the aircraft noise model FLULA2 with CNOSSOS. Additionally, calculation results of both models are compared to each other and corresponding measurements. FLULA2 and CNOSSOS are both models yielding A-weighted noise metrics that combine sound emission and propagation for the determination of the noise exposure at receiver positions on the ground. However, the modelling approaches of FLULA2 and CNOSSOS are inherently different, which requires a systematic comparison. As both modelling approaches do not consequently distinguish between sound emission and propagation phenomena, the comparisons focus on sound exposure level at receiver positions on the ground. For quantitative comparisons, calculations with the Aviation Environmental Design Tool (AEDT), issued by the U.S. Federal Aviation Administration (FAA), are used [4]. While, strictly speaking, AEDT is not a CNOSSOS compliant model, it is a CNOSSOS equivalent model on airport scale (i.e., for calculations of complex yearly air traffic scenarios with many flights) and thus suited for the current comparisons. **In the following, we refer to CNOSSOS also in cases where results of calculations with AEDT are presented.**

The report is structured as follows: Section 3 describes the methodology of the comparison of the two models with each other and with measurement data. Further, the origin of the input data used for the calculations is briefly described. In Section 4, the modelling approaches and basic formulas of the two models are compared with each other. Additionally, a detailed tabular overview of both models is given. Section 5 documents calculation results performed with the two models. The sound exposure levels for several thousand single flights of commercial aircraft at Zurich and Geneva airports, Switzerland, which were obtained in a previous project, CompAIR [8], are presented. Comparisons of the results obtained with CNOSSOS using default input parameters (in accordance to the default values of the Commission Directive (EU) 2015/996 [10]) are presented in Section 5.1, and exemplary results using input data (flight profiles and NPD data) adjusted to the conditions of Swiss airports in Section 5.2. In Section 6, the main findings are discussed and conclusions are given.

3. Methodology and underlying data

3.1. Overview

The aircraft noise calculation model FLULA2 and CNOSSOS are both best practice noise calculation models developed to determine averaged A-weighted noise metrics resulting from complex scenarios consisting of many flights (e.g., yearly air operations). Both models combine sound emission and propagation calculation to directly determine the noise exposure at a given set of receiver locations. As their modelling approaches differ inherently – for example, FLULA2 uses a time-step and CNOSSOS a segmented model approach (see, e.g., [3]) – the models are compared regarding (i) their modelling approaches and basic noise calculation formulas and equations (covered in Section 4, including a tabular overview in Table 4-1) and (ii) the calculated noise exposure (sound exposure levels, L_{AE}) at given receiver positions (Section 5). Thus, the quantitative comparisons implicitly include the sound emission and propagation calculations of both models, as the respective results cannot be separated from each other. Modelling results of FLULA2 and CNOSSOS are compared with each other as well as to corresponding noise measurements. This is conducted for a large set

of single flights of commercial aircraft at Zurich (ZRH) and Geneva (GVA) airports. Besides calculations with AEDT using default input data, NPD data are exemplarily adjusted to local conditions around Zurich airport for two narrow-body aircraft types.

3.2. Measurement data

The underlying measurement data originate from measurements in the years 2017 and 2018 used for validation purposes of the aircraft noise calculation model sonAIR [23, 24], where calculated sound exposure levels L_{AE} of individual flights were compared with acoustic measurements obtained from noise monitoring terminals (NMTs) at Zurich and Geneva airports. As model calculation inputs, radar and flight data recorder (FDR) data, airport data (e.g., runways, terrain) and sound source data were used (details see [15]).

The noise exposure data for comparisons within the present report have been adopted from the project CompAIR [8], where Empa performed comparative calculations with three models, namely FLULA2, AEDT as the CNOSSOS equivalent program, and sonAIR (not treated here), for Zurich and Geneva airports.

In short, the data set covers 8'390 single flights (Table 3-1) of 27 turbofan aircraft types (partly with different engines: Table 3-2). Data from 18 measurement locations were analyzed, covering all main departure and approach routes at distances from 1.8 to 10 kilometers from the airports (Figure 3-1). Details on the data set can be found in [8, 15].

Table 3-1: Number of simulated flights and aircraft types

FDR available	No. of flights	Airport(s)	No. of different aircraft types
yes	1'732	Geneva / Zurich	8
no	6'658	Geneva / Zurich	24

Table 3-2: Simulated aircraft types (ICAO designation) with FDR data or with radar data available. For several types, both cases occurred.

Aircraft types with available FDR data	A319, A320, A321, A333, A343, B77W, BCS1, BCS3
Aircraft types without available FDR data	A319, A320, A321, A333, A343, A388, B733, B734, B735, B736, B737, B738, B739, B762, B763, B764, CRJ7, CRJ9, CRJX, E170, E190, E195, F100, FA7X

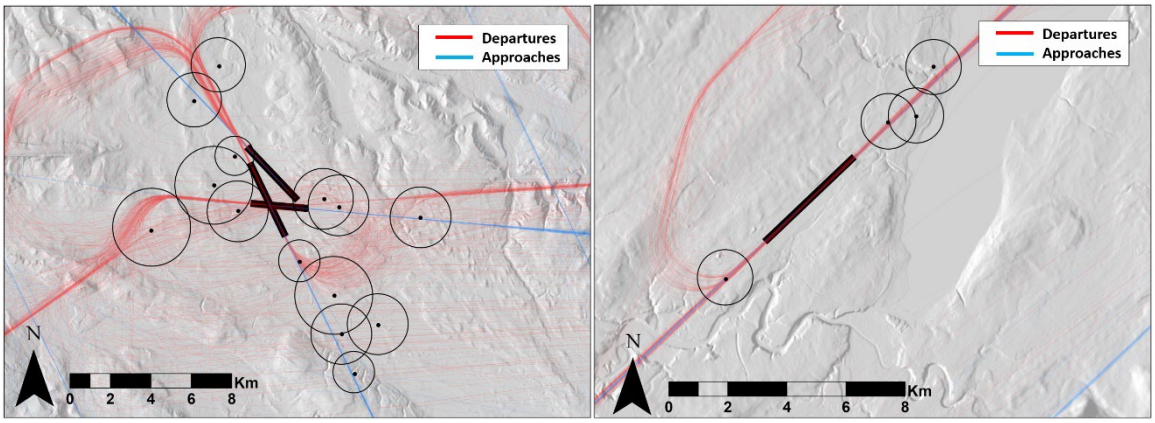

Figure 3-1: **Noise monitoring terminals (NMT) in the vicinity of Zurich (left) and Geneva airport (right) with all flight trajectories used within the present study, colored by procedure. The black circles around each terminal represent spatial gates, which the flight trajectories had to penetrate to be considered. Basemap: swissALTI3D LV95; source: Federal Office of Topography (swisstopo). Figures taken from [18] (CC BY 4.0, https://creativecommons.org/licenses/by/4.0/)**

3.3. Comparisons

Within this study, the noise exposure calculations with FLULA2 and CNOSSOS are compared with each other and with corresponding measurements. The focus of the comparison is on the A-weighted sound exposure level L_{AE} of individual flights at different propagation distances and positions with respect to the aircraft. Specifically, the $L_{AE,tg}$ is used in the measurements to have a sufficiently large signal-to-noise ratio to exclude background noise, with tg being the time period of an event with the instantaneous sound pressure level above a NMT specific threshold (Zurich airport) or dynamic threshold (Geneva airport). For CNOSSOS the L_{AE} (complete event) and for FLULA2 the $L_{AE,t10}$ is used, where t10 is the 10 dB-down-time (time period during which the sound pressure level is not more than 10 dB below the maximum sound pressure level, $L_{AS,max}$). While FLULA2 can determine the $L_{AE,t10}$ (closely corresponding to $L_{AE,tg}$), which was used for optimal comparability with measurements, AEDT does not yield the $L_{AE,t10}$ as output, but only the L_{AE}. However, the L_{AE} in the AEDT database (NPD data) are based on 10dB-down-time values (p. L 168/70 in [10]). Also, the difference between $L_{AE,t10}$ and L_{AE} is usually small (in the range of some 0.1 dB). Thus, all three quantities, the measured $L_{AE,tg}$ and calculated $L_{AE,t10}$ (FLULA2) and L_{AE} (CNOSSOS) are highly comparable.

Corresponding calculations of the maximum sound pressure level $L_{AS,max}$ can be found in the Annex (Section 8). In addition to CNOSSOS calculations with default input data, comparisons are made with input data for CNOSSOS that are adapted to local average conditions around Zurich and Geneva airports. For this purpose, exemplarily NPD data plus fixed-point profiles adjusted to local conditions around Zurich airport are generated for two narrow-body aircraft types, as representatives for similar aircraft types.

4. Model comparison

The aircraft noise calculation model FLULA2 used for official calculations in Switzerland and the CNOSSOS model are both best practice aircraft noise calculation models developed to determine averaged A-weighted noise metrics (e.g., L_{Aeq}, L_{den}) resulting from complex scenarios consisting of many flights (e.g. yearly air operations).

Both models combine sound emission and propagation calculation to determine the noise exposure at a given set of receiver locations. Detailed descriptions of FLULA2 can be found in [6, 16]. CNOSSOS is fully described in the Commission Directive (EU) 2015/996 [10, 12]; it closely corresponds to ECAC Doc.29 [5] and ICAO Doc.9911 [13]. A concise overview on the modelling approach is given in [14]. For the current calculations, we used FLULA2 Version 004 and – as a CNOSSOS equivalent program on airport scale – AEDT Version 3d [4]. In Sections 4.1 and 4.2, the modelling approaches and input data of FLULA2 and CNOSSOS (AEDT) are described and compared. Table 4-1 in Section 4.3 provides an overview of the main similarities and differences of the two models, and Section 4.4 describes the methodology to adjust input data for CNOSSOS to local conditions.

4.1. FLULA2

FLULA2 is a time-step aircraft noise calculation model, used in Switzerland for official noise calculations at Zurich and Geneva airports. It is an "immission model" [3], which, contrary to emission models, directly outputs the sound exposure level at a given receiver location. Sound emission and propagation are thus combined in the noise exposure calculation. The sound source (emission strength and directivity) plus propagation (geometric divergence and atmospheric absorption) is described by an empirical formula describing the instantaneous A-weighted sound pressure level (L_A) as a function of the emission angle θ relative to the flight path and the distance r between sound source and receiver (Figure 4-1).

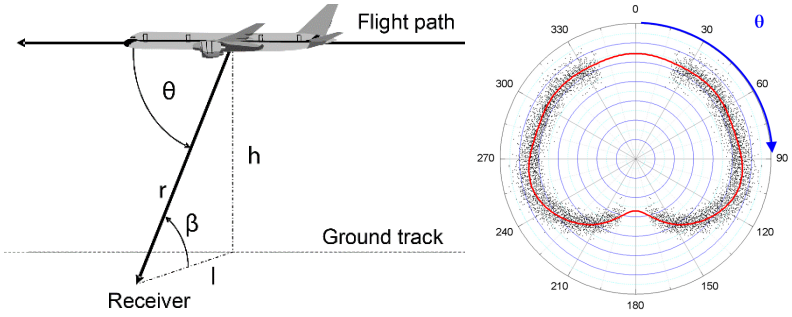

Figure 4-1: **Left: Geometric relation between sound source and receiver (left), with aircraft height *h*, lateral distance *l*, distance *r* between sound source and receiver emission, emission angle θ relative to the flight path, and elevation angle β. Right: Exemplary sound directivity pattern for instantaneous A-weighted sound pressure level (L_A) as a function of the emission angle θ relative to the flight path for an A320 during departure at a distance of 1'000 ft (right, taken from [6]).**

The A-weighted sound pressure level for a discrete aircraft position at an arbitrary receiver location is described by Formula 4–1. For each aircraft type and procedure – takeoff with maximum power; takeoff with reduced power; landing – , a set of 32 H_{ik} coefficients is available. Details on the modelling approach and

interpretation of the coefficients are given in [16]. With these coefficients and the propagation geometry (θ,r), the corresponding instantaneous sound exposure level L_A at the receiver point per aircraft type and procedure is obtained. The modelling approach assumes that the sound emission is rotationally symmetrical with respect to the flight axis, i.e., that there is only a longitudinal directivity and that engine installation effects (lateral directivity) are thus negligible. The directivity patterns are fixed for each aircraft type and the above mentioned procedures.

Formula 4-1 $L_A(\theta, r) = \sum_{i=0}^{7}(H_{i1} \cdot 20\lg(r) + H_{i2} + H_{i3} \cdot r + H_{i4} + r^2) \cdot cos^i(\theta)$; for $r \leq$ 4500m

The function $L_A(\theta,r)$ describes the directional and distance dependent A-weighted sound pressure level for standard atmospheric conditions (15°C, 1013 hPa and 70% rel. humidity). The formula implicitly includes the frequency dependent sound emission and the frequency dependent atmospheric attenuation to yield the $L_A(\theta,r)$ on the ground. Since Formula 4–1 diverges for large distances r, the sound propagation is calculated with the Formula 4–2 for distances greater than the limit distance $r_{boundary}$ of 4'500 meters.

Formula 4-2 $L_A(r, \theta) = L_A(r_{boundary}, \theta) - 20 \cdot \lg\left(\frac{r}{r_{boundary}}\right) - b \cdot (r^m - r_{boundary}^m)$; for r > 4'500m

The parameters b and m are determined for each aircraft type and procedure (takeoff with maximum and reduced power; landing) from the H_{ik}-coefficients at the distance $r_{boundary}$ of 4'500 m (details see [6]).

To account for different operating conditions during takeoff (cutback) and landing (power reduction for some aircraft types on the runway), specific level corrections (ΔL) are defined which describe the change of sound pressure level with respect to the initial level of the sound source model (Formula 4–1). The ΔL (for details and values see [6]) are added to the L_A resulting from Formula 4–1 and consequently do not change the directivity of the source model.

To account for lateral attenuation effects at small angles of sound incidence, an additional empirical term is used (Formula 4–3).

Formula 4-3
$\Delta L(\beta, r) = [1 - 3.8637 \cdot \sin(\beta)] \cdot (10.1451 - 9.9 \cdot e^{(-0.00134 \cdot r)})$; for β < 15°
$\Delta L(\beta, r) = 0$; for $\beta \geq$ 15°

Formula 4–3 combines access attenuation due to ground effects and meteorological effects, where β represents the elevation angle and r the slant distance between source and receiver. The modelling approach is similar to CNOSSOS. However, other empirical coefficients are used. Further, the angle β is defined by the "free area" between the connecting line of source to receiver and the ground as obtained from terrain slices. The angle β thus accounts for the actual terrain and does not assume a flat terrain. For flat terrain, the method yields the same β as the definition of CNOSSOS, but different elevation angles in hilly terrain. As an example, in a situation where a receiver is on a mountain top and an airplane laterally passes by at the same altitude, CNOSSOS would yield β = 0° and thus maximum lateral attenuation, while the FLULA2 method

would yield $\beta >> 0°$ (reduced or no lateral attenuation), which is physically more sound. Details of the determination of β can be found in [6]. The attenuation resulting from the lateral attenuation is shown in Figure 4-2. Formula 4–3 yields attenuation values of up to 10 dB.

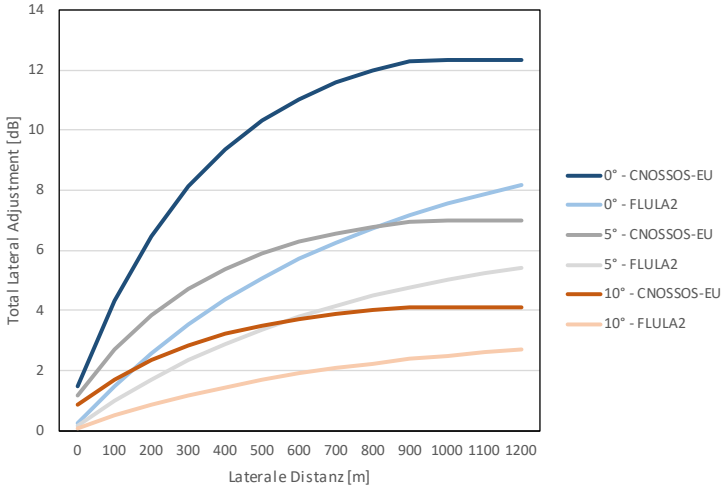

Figure 4-2: **Lateral attenuation as a function of the lateral distance and the elevation angle β in FLULA2 [6] and in CNOSSOS for civil wing-mounted aircraft [10, 12] (the latter taken from SAE AIR 5662 [20]; cf. Section 4.2). While CNOSSOS defines different engine installation effects for wing-mounted and fuselage-mounted aircraft, FLULA2 does not distinguish between these two. Lateral attenuation for fuselage-mounted aircraft is not shown here as no such aircraft are modelled in this study.**

Shielding to account for barrier effects is described by a "quasi-optical model with gentle fade" [17]. The attenuation is calculated as a function of the "shadow area", which is defined as the area of the terrain profile above the connecting line of source to receiver. Per 1000 m^2 of shadow area, the additional attenuation amounts to ~0.9 dB.

FLULA2 is able to consider three-dimensional fixed-point flight trajectories of any shape with aircraft position (x, y, h) and aircraft speed in discrete time steps (usually 1 s), obtained, e.g., from radar data [22]. The energetic contribution of each aircraft point along a trajectory to the L_{AE} at a certain receiver position is energetically summed up to obtain the L_{AE} (or $L_{AE,t10}$) of the whole flight. Thereafter, the contribution of multiple flights to an overall exposure (e.g., L_{den}) is obtained from all single events.

4.2. CNOSSOS

In this section, we describe the CNOSSOS model according to the Commission Directive (EU) 2015/996 [10, 12]. While we used AEDT as a CNOSSOS equivalent program implementation, all considerations apply for both, CNOSSOS and AEDT. The remaining subtle differences between the two models will hardly have a relevant influence on the calculation results for the present situations. A concise model description is given in [14]. CNOSSOS is an integrated or segmented model [3], which breaks down the flight path into several segments with variable power and speed to model straight and curved flight paths. As FLULA2, it is an "immission model" [3] which directly calculates the sound pressure level at the receiver position and thus combines sound emission and propagation. The sound emission plus propagation (geometric divergence

and atmospheric absorption) are modelled with "Noise-Power-Distance" (NPD) data for infinite path lengths. These contain sound exposure levels (L_{AE}) as a function of thrust (power) and distance to the receiver. The values are given for standard atmospheric conditions according to SAE-AIR-1845 [19], although they can also be adjusted to the conditions of the ISA Standard Atmosphere or local conditions. Performance (power) calculations are done using the ISA standard atmosphere (see AEDT Technical Manual [4], chapter 11.2.3.1.2, Table 11-14). NPD data are given specifically per aircraft type, procedure and noise metric (maximum event level $L_{AS,max}$, single event level L_{AE} etc.). The calculation is based on the assumption that the sound exposure produced by a flight path segment of finite length can be derived from the exposure produced by an infinite path using a so-called "energy fraction". For the segment-by-segment noise calculation of a flight, the individual values of the NPD data are interpolated.

To account for the longitudinal directivity, a fourth-power 90-degree dipole is assumed. It is used in the energy fraction to obtain the so-called "finite segment correction" Δ_F [10]. For lateral directivity, an engine installation correction (referred to as "engine installation effects"; for wing-mounted and fuselage-mounted aircraft) is applied (cf. Figure 2.7.n of the Commission Directive (EU) 2015/996 [10]). For civil wing-mounted aircraft which are studied here, lateral directivity amounts to +0.4 dB to –1.5 dB, depending on the roll axis angle Φ, compared to the reference angle at Φ = 0° directly below the aircraft.

As in FLULA2, an empirical lateral attenuation term is used to account for situations with small angles of sound incidence (Formula 4–4). However, another approach is used for CNOSSOS, according to SAE AIR 5662 [20]. Note that while the Commission Directive (EU) 2015/996 separately presents two terms, a distance factor $G(l)$ plus a long-range air-to-ground lateral attenuation $A_{GRD+RS}(\beta)$, these two terms add up to Formula 4–4 in the so-called "transition region" [20]) which has the same structure as in FLULA2. Additionally, the term $E_{Eng}(\varphi)$ describes engine installation effects (see above).

Formula 4-4 $\Lambda(\varphi, l, \beta) = E_{Eng}(\varphi) - \frac{G(l) \cdot A_{GRD+RS}(\beta)}{10.86}$

In Formula 4–4, β again describes the elevation angle and *r* the distance between source and receiver. In contrast to FLULA2, flat terrain is assumed to determine β. The attenuation resulting from the lateral attenuation is shown in Figure 4-2. With maximum values of almost 12.4 dB, substantially larger attenuations result than with FLULA2.

Contrary to FLULA2, shielding effect is not accounted for. While this simplification is justified for sufficiently flat terrain, it would be problematic for hilly or mountainous regions like in the Swiss alps. However, the situations studied here (departures and approaches around Geneva and Zurich airports) are not critical with respect to barrier effects. (Note that while AEDT would allow accounting for line-of-side blockage, it remained unaccounted for present report, to be compliant with CNOSSOS.)

Accounting for 3D flight trajectories is somewhat less straight forward than in FLULA2. Not only altitude and speed profiles are needed, but also the power setting. Therefore, radar data cannot be used directly for the noise calculations. Usually, the flight tracks can be used, but the profiles are obtained from default or adjusted procedural flight profiles. Such profiles describes altitude, speed and thrust as a function of the height

above ground (cf. default procedural steps according to Table I-3 in [10]). Adjusting these procedural profiles to local conditions is not straightforward (cf. Section 4.4), particularly when establishing from radar data, due to the lack of information on thrust. Therefore, one may use fixed point profiles giving a set of height, speed and thrust values as a function of ground distance. Three-dimensional trajectories are then formed from the profiles and flight tracks and subdivided into a sequence of straight-line segments by means of segmentation. The energetic contributions of the segments (i.e., partial flight tracks) to the noise exposure levels are determined separately (energy fractions) and energetically summed up to obtain the L_{AE} of the flight. Thereafter, the contribution of all flights to an overall exposure (e.g., L_{den}) is calculated from all single events.

4.3. Similarities and differences between FLULA2 and CNOSSOS

Table 4-1 compares the most important properties of FLULA2 and CNOSSOS to emphasize the similarities and differences between the two models.

Table 4-1: Detailed tabular model comparison between FLULA2 and CNOSSOS

Topic	FLULA2	CNOSSOS
General		
Model approach	Time step model	Segmented model / noise fraction
Noise calculation method	Combined sound emission and propagation in empirical sound emission patterns	Combined sound emission and propagation using noise power distance (NPD) data
Aircraft categories	Specific aircraft types (no discrimination between engines), own designations, largely comparable to ICAO designations	Specific aircraft and engine types, ICAO designations
Data basis		
Emission data	Measurements by Empa on real air traffic around Zurich airport	Noise power distance (NPD) data obtained from noise certification data
Flight trajectories	Position (x, y) altitude above ground (h), speed (v) in discrete time steps (usually 1 s), obtained from radar data or idealized flight trajectories (track plus profiles)	Position (x, y) altitude above ground (h), speed (v) and thrust (P) per flight path segment. Segments obtained with a seg-mentation approach and flight performance calculations (Appendix B of [10, 12]) from tracks (radar data or idealized) and flight profiles (procedural or fixed point)
Noise emission modelling		
Spectral or integral calculation	Integral, A-weighted sound pressure level	Integral, A-weighted sound pressure level
Source directionality	2D (longitudinal directivity, aircraft specific)	3D (2D dipole directivity, adapted to scaled distance + engine installation effects)
Sound propagation		
Sound propagation phenomena	Geometric divergence, atmospheric absorption, lateral attenuation, shielding (line-of-side blockage)	Geometric divergence, atmospheric absorption, lateral attenuation
Atmospheric conditions	ISA standard atmosphere	ISA standard atmosphere used here (could also use other atmospheric conditions)
Atmospheric attenuation	ISO 9613-1 (used to develop the model according to Formula 4–1)	SAE-ARP-5534 used here (could also use SAE-ARP-866A or SAE-AIR-1845)
Terrain model	Yes (here: DHM25 from swisstopo)	No (but receiver height above non-flat terrain is accounted for, see below)
Ground conditions	Soft ground	Soft ground
Lateral attenuation correction	Yes (empirical correction for phenomena under low sound incidence [6])	Yes (empirical correction for phenomena under low sound incidence [10])
Shielding effect	Yes, from terrain	No
Consideration of buildings	No	No
Reflections (except ground)	No	No

Topic	FLULA2	CNOSSOS
Sound exposure		
Receiver height	Freely selectable. Here: terrain height + 4 m	Freely selectable. Here: terrain height + 4 m
Grid structure:	Selectable mesh size	Selectable mesh size
Noise metrics (simulation)	L_{AE}, $L_{AE,t10}$, L_{Amax} (other metrics also available)	L_{AE}, L_{Amax} (other metrics also available)
Noise contours generation	2D-B-Spline (second degree B-spline algorithm)	Linear interpolation (with local grid refinement), see Sec. 2.7.26. to 2.7.28 in [10].

4.4. Adjustment of CNOSSOS default data to local conditions

There are several options for adapting the input data of CNOSSOS to local conditions. For example, one can use real weather and terrain data, adapt the flight profiles or adjust the noise power distance (NPD) data. In our experience, the last two points have the greatest influence on the noise calculation. The default data is therefore adjusted by using real flown flight profiles as "fixed point profiles" and by adjusting the underlying NPD data.

In a recent update of FLULA2, sound source data for a range of aircraft were established from sonAIR sound emission data. The latter were obtained from measurements on Zurich airport [23, 24]. These measurements represent the local conditions (local aircraft fleet) well and can be used to generate adjusted NPD data. For this purpose, we performed "pseudo-certification flights" with sonAIR (as sonAIR uses N1 as a proxy for performance as input parameter, which is needed in CNOSSOS calculations) according to the reference conditions in chapter 2.7.6. of [10] at the same overflight altitudes as given in the NPD data (200–25'000 ft, cf. Table I-9 in Commission Directive (EU) 2015/996 [10]). The microphone position was set to 4 m above ground, and the minimum elevation angle of the aircraft to 10°; both settings largely avoid unwanted ground effects. An illustration of these certification flight simulations is given in Figure 4-3. Since the sonAIR aircraft noise model depends on airspeed, real mean airspeeds were used for the certification flights and scaled to the prescribed reference speed for certification flights of 160 knots.

sonAIR uses the engine's low-pressure rotational speed N1 as performance input parameter instead of thrust [24]. Therefore, we replaced the thrust values in the NPD data with N1 values, which results in "NN1D tables " (noise N1 distance tables). Using these NN1D tables, flight trajectories with N1, which were available from CompAIR [8], could directly be used in the CNOSSOS (AEDT) noise calculations within the present study. A separate thrust calculation as for standard calculations with CNOSSOS, was therefore not necessary.

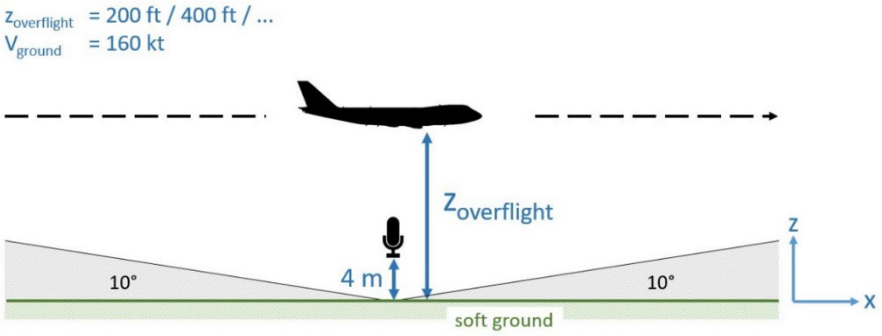

Figure 4-3: Methodological approach to obtain " NN1D tables" (noise N1 distance tables) from simulations with sonAIR.

5. Single flights noise calculation results

In the following, the results of the single flights noise exposure calculations are compared between the two models as well as with the measurements. First, the results of FLULA2 and CNOSSOS with default input data are shown (section 5.1). Exemplary results of CNOSSOS with adjusted input data (profiles and NN1D tables) are shown in section 5.2. The comparison with the measurements from Zurich and Geneva airports are shown in pooled form. The acoustic quantities used for the comparison are the A-weighted sound exposure level L_{AE}, $L_{AE,t10}$, and $L_{AE,tg}$ (cf. Section 3.3). Corresponding results with $L_{AS,max}$ can be found in the Annex (Section 8).

The following Figure 5-1 and Figure 5-2 are arranged as follows: The graph on the left shows a scatter plot comparing the simulated L_{AE} or $L_{AE,t10}$ (y-axis) with the measured $L_{AE,tg}$ (x-axis). The results are separately presented for departures and approaches. Further, the scatter plot shows the key figures such as the number of events and flights, the mean and median values of the differences between simulation and measurements (calculations minus measurements), where positive values indicate an overestimation of the measurements by the model calculation, and the standard deviations (SD) of the differences between calculation and measurements. The right graph shows boxplots of the differences between calculations and measurements, split by departures and approaches. The single scatter plot in Figure 5-3 shows a direct comparison of the calculated noise levels of FLULA2 and CNOSSOS (difference FLULA2 minus CNOSSOS), hence without the measurement values.

5.1. Comparison of FLULA2 and CNOSSOS with default settings

Overall, the noise exposure levels $L_{AE,t10}$ calculated with FLULA2 agree well with the measurements (Figure 5-1). Both the departures and approaches are represented well, resulting in an overall mean deviation between simulation and measurement of +0.1 dB. The overall standard deviation is 2.2 dB.

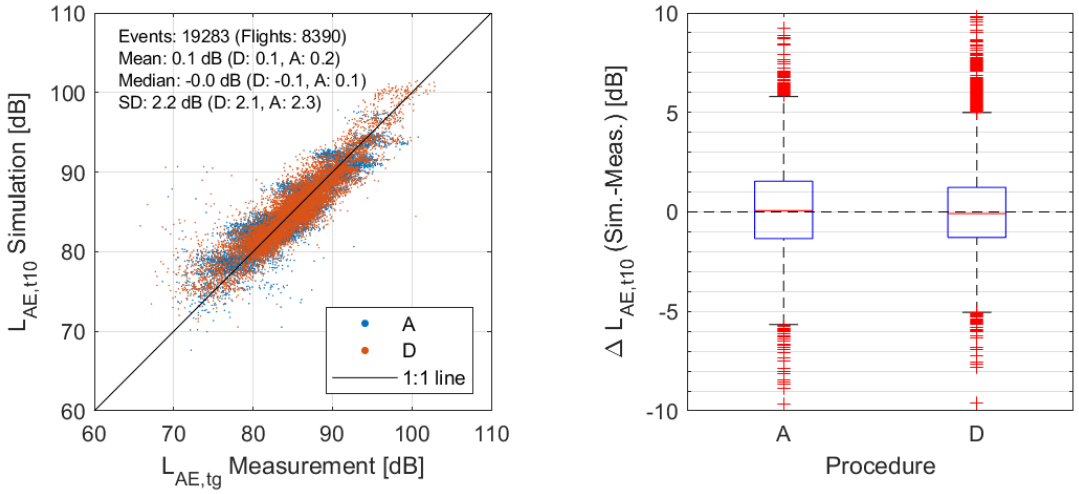

Figure 5-1: Scatter plot (left) and boxplot (right) of the calculated $L_{AE,t10}$ (FLULA2) with the measurements in the vicinity of Zurich and Geneva airports, grouped by departures and approaches.

The noise exposure levels L_{AE} calculated with CNOSSOS also agree well with the measurements, with a mean difference between simulation and measurements of –0.4 dB and an overall standard deviation of 2.5 dB (Figure 5-2). The agreements to measurements are thus on average quite similar to FLULA2, but approaches

are generally slightly overestimated (+0.4 dB) and departures somewhat more underestimated (–1.1 dB; Figure 5-2).

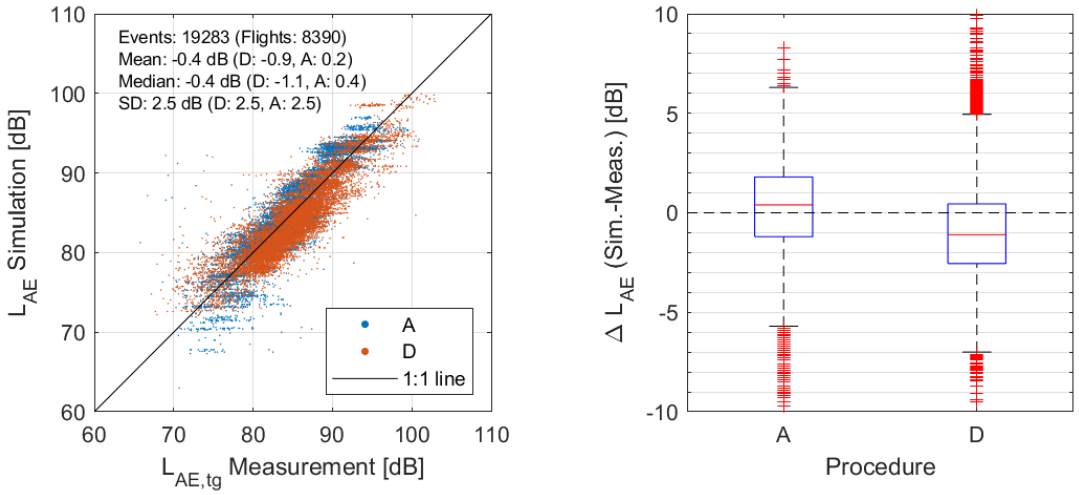

Figure 5-2: **Scatter plot (left) and boxplot (right) of the calculated L_{AE} (CNOSSOS) with the measurements in the vicinity of Zurich and Geneva airports, grouped by departures and approaches.**

In both scatter plots (Figure 5-1, Figure 5-2), horizontal groupings are visible (very similar $L_{AE,t10}$ or L_{AE} values within a range of measured values). For FLULA2, this can be explained by its rigid sound source models, particularly for approaches of the same aircraft type with similar trajectories at certain receiver locations. For CNOSSOS, it can be explained by type-specific standard procedural profiles for the present calculations, in which the thrust and altitude profile and thus the L_{AE} at a given location is very similar for a large number of flights. Especially for less noisy approaches, some aircraft type-specific deviations can be clearly identified as horizontally layered clusters.

Furthermore, the scatter plot in Figure 5-2 shows distinct underestimations of the measured L_{AE} for landings in the range of simulated L_{AE} below 70 dB. The (grouped) differences of these events are aircraft type and measurement location specific and again due to the use of standard procedural profiles, which are not able to adequately represent the corresponding events equally well. This can be improved by adjusting input data to the specific airport (see Section 5.2).

Figure 5-3 compares the $L_{AE,t10}$ simulated with FLULA2 with the L_{AE} simulated with CNOSSOS to reveal how well the model calculations agree. Overall, the noise exposure values agree well, with a mean difference of +0.5 dB (FLULA2 minus CNOSSOS), a standard deviation of 2.3 dB and the data roughly following the 1:1 line. Some individual groups ("bands") above 90 dB on the x-axis with larger deviations are identifiable for departures. This may be due to aircraft type or measurement location specific differences between the two models. Overall, however, there are no systematic differences between these two models, so that their computational results are equivalent on average. This is crucial, as both programs were developed and are used to calculate averaged noise exposures of yearly air traffic (i.e., complex scenarios of many aircraft types on many air routes).

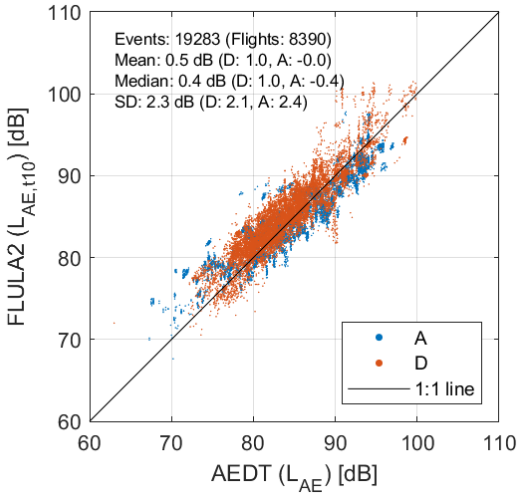

Figure 5-3: **Scatter plot of the calculated $L_{AE,t10}$ of FLULA2 with the calculated L_{AE} of CNOSSOS in the vicinity of Zurich and Geneva airports, grouped by departures and approaches.**

5.2. Comparison of FLULA2 and CNOSSOS with adjusted input data

Figure 5-4 and Figure 5-5 show exemplary calculations with CNOSSOS using default input data and corresponding results after adjusting the input data to local conditions around Zurich airport (Section 4.4) for two narrow-body aircraft types, which were selected as they tended to perform less well than the other aircraft types in the previous section. CNOSSOS represents the measurements substantially better after the adjustment. While the unadjusted data show a mean difference of –1.6 dB with a standard deviation of 2.1 dB, the adjusted data have a mean difference of +0.3 dB with a standard deviation of 1.8 dB. Also, the adjusted data now closer follows the 1:1 line. Further, the grouping ("bands") of approaches due to the aircraft type-specific standard procedural profiles (Figure 5-4) is substantially reduced with the use of adjusted profiles for the two aircraft types (Figure 5-5).

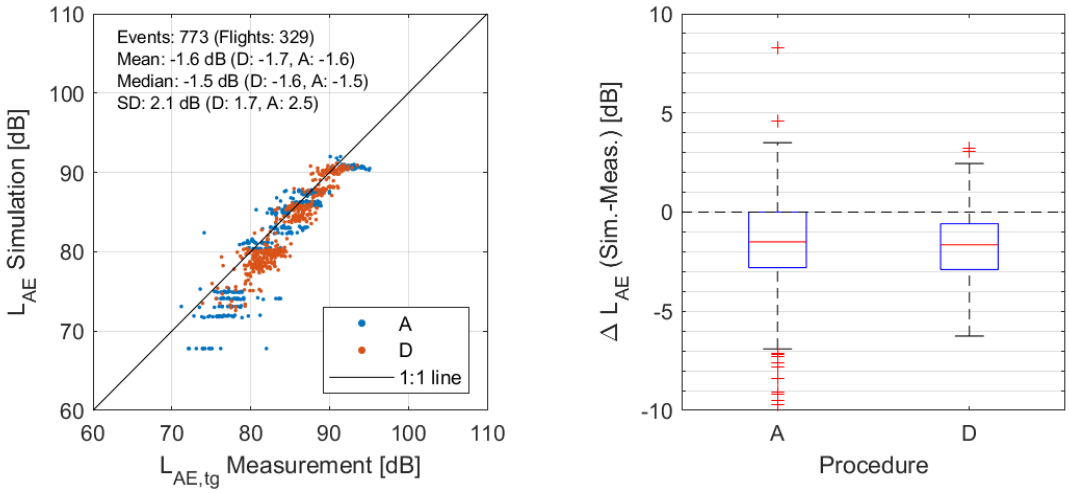

Figure 5-4: **Scatter plot (left) and boxplot (right) of CNOSSOS calculations with default input data: Comparisons of the calculated L_{AE} with the measurements in the vicinity of Zurich airports for two exemplary narrow-body aircraft types, grouped by departures and approaches.**

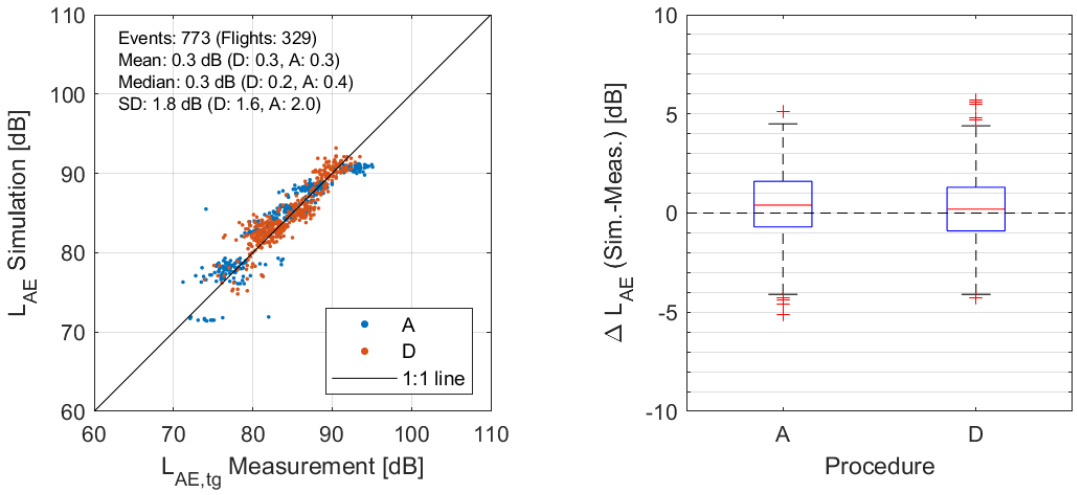

Figure 5-5: **Scatter plot (left) and boxplot (right) of CNOSSOS calculations with adjusted input data: Comparisons of the calculated L_{AE} with the measurements in the vicinity of Zurich airports for two exemplary narrow-body aircraft types, grouped by departures and approaches.**

Figure 5-6 compares the agreement between CNOSSOS and FLULA2 (difference FLULA2 minus CNOSSOS) before and after the adjustment of the input data. As expected, with adjustment, the modelling results of the two models agree substantially better than without. The mean difference (standard deviation) is +1.2 dB (1.9 dB) before and –0.7 dB (1.1 dB) after adjustment. Also, the adjusted calculations follow the 1:1 line much closer than the unadjusted data.

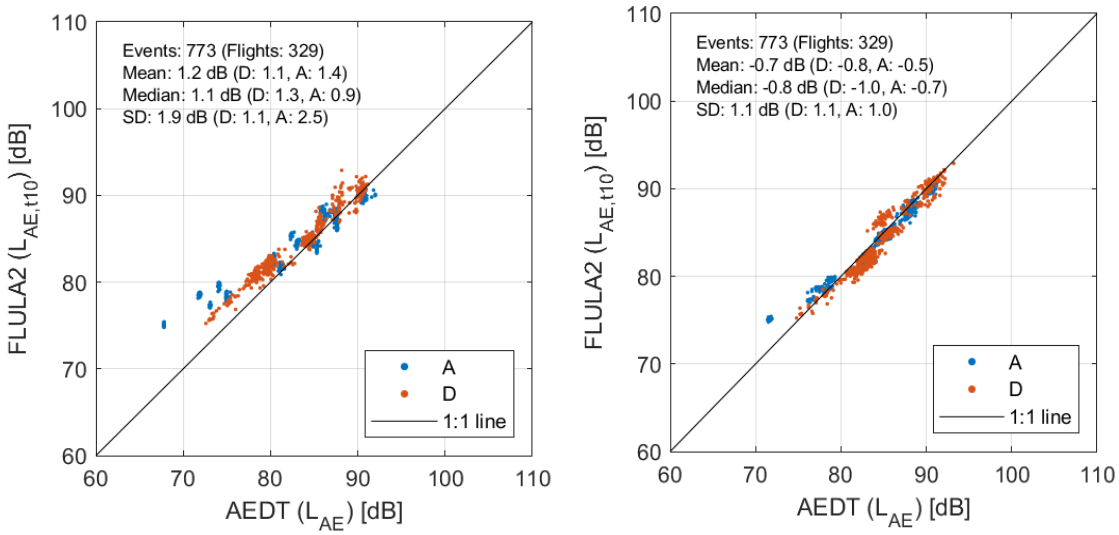

Figure 5-6: **Scatter plot of $L_{AE,t10}$ calculated with FLULA2 in comparison to L_{AE} calculated with CNOSSOS with default (left) and adjusted (right) input data for two exemplary narrow-body aircraft types,.**

6. Conclusions

In this study, the Swiss aircraft noise model FLULA2 and the European model CNOSSOS were compared formally with respect to their methodological approaches and input data, and by calculating 8'785 single flights around Zurich and Geneva airports to compare the modelling results with each other as well as with measurement data, to test whether FLULA2 conforms with CNOSSOS. While FLULA2 and CNOSSOS use disparate modelling approaches, these differences only moderately affected the calculated results.

For noise exposure calculations with FLULA2, a mean difference of +0.1 dB with a standard deviation of 2.2 dB between calculations and measurements for the $L_{AE,t10}$ was found, while CNOSSOS (using default input data) yielded a mean difference of –0.4 dB with a standard deviation of 2.5 dB for the L_{AE}. Thus, both models achieved a good overall performance in reproducing measurements. Further, results also agree well between models, with a mean difference of +0.5 dB (FLULA2 minus CNOSSOS) and a standard deviation of 2.3 dB.

The agreement between the models may even be improved if the input data for CNOSSOS (NPD data, flight profiles) are adjusted to local conditions. Exemplary calculations for departures and approaches of two narrow-body aircraft types around Zurich Airport showed an improved agreement with measurements, with the (absolute) mean difference decreasing from –1.6 dB (standard deviation of 2.1 dB) to +0.3 dB (standard deviation of 1.8 dB). Also the differences (FLULA2 minus CNOSSOS) between modelling results of FLULA2 and CNOSSOS decreased, from +1.2 dB (standard deviation of 1.9 dB) to –0.7 dB (standard deviation of 1.1 dB).

The current comparisons are based on measurements obtained from noise monitoring terminals representative for areas with legally relevant noise exposure. Slightly different results would be obtained for other situations, but the resulting differences between models and measurements are likely remain small. Only in situations with larger propagation distances and/or grazing sound incidence larger differences may occur, but such situations are usually at lower sound exposures.

Thus, FLULA2 on average yields very similar results as CNOSSOS, with average differences below 1 dB, and there are no systematic differences between modelling results. Given the uncertainty of aircraft noise calculations which will be in the range of 0.5 to 1.0 dB for complex scenarios [21], the differences between the models are not significant, and the results thus can be regarded as equivalent.

This leads to the conclusion that FLULA2 is equivalent to CNOSSOS on the airport scale, i.e., when used to calculate averaged noise exposures of yearly air traffic (complex scenarios of many aircraft types on many air routes), which is the primary aim both models are designed for.

7. References

[1] BAFU, 2021. *Webpage: Ermittlung und Beurteilung von Fluglärm*. Bundesamt für Umwelt (BAFU), Bern. URL: https://www.bafu.admin.ch/bafu/de/home/themen/laerm/fachinformationen/laermermittlung-und--beurteilung/ermittlung-und-beurteilung-von-fluglaerm.html.

[2] BAFU, BAZL, und GS-VBS, 2016. *Leitfaden zur Fluglärmermittlung. Vorgaben für die Lärmermittlung. Umwelt-Vollzug Nr. 1625*. Bundesamt für Umwelt (BAFU), Bundesamt für Zivilluftfahrt (BAZL), Generalsekretariat des Eidg. Departementes für Verteidigung, Bevölkerungsschutz und Sport VBS (GS VBS), Bern. URL: http://www.bafu.admin.ch/bafu/de/home/themen/laerm/publikationen-studien/publikationen/leitfaden-fluglaerm.html.

[3] Bütikofer, R., 2007. *Concepts of aircraft noise calculations.* Acta Acustica united with Acustica **93**, 253-262.

[4] DOT, 2021. *Aviation Environmental Design Tool (AEDT), Version 3d, Technical Manual*. U.S. Department of Transportation (DOT), Volpe National Transportation Systems Center, Cambridge, MA 02142. URL: https://aedt.faa.gov/Documents/AEDT3d_TechManual.pdf.

[5] ECAC, 2016. *ECAC.CEAC Doc 29: Report on Standard Method of Computing Noise Contours around Civil Airports, Volume 2: Technical Guide. 4th ed.* European Civil Aviation Conference (ECAC), Neuilly-sur-Seine, France. URL: https://www.ecac-ceac.org/documents/ecac-documents-and-international-agreements.

[6] Empa, 2010. *FLULA2, Ein Verfahren zur Berechnung und Darstellung der Fluglärmbelastung. Technische Programm-Dokumentation. Version 4*. Eidgenössische Materialprüfungs- und Forschungsanstalt (Empa), Abteilung Akustik / Lärmminderung, Dübendorf. URL: http://www.empa.ch/web/s509/flula2 (zuletzt besucht: 14.04.2019).

[7] Empa, 2019. *Conformity of the Swiss railway noise emission model sonRAIL with CNOSSOS-EU*. Swiss Federal Laboratories for Materials Science and Technology (Empa), Laboratory for Acoustics / Noise Control, Dübendorf.

[8] Empa, 2021. *Vergleich der mit den Modellen FLULA2, AEDT und sonAIR berechneten Immissionspegel von Einzelflügen mit Messungen.* Bericht Nr. 5211.01812.100.01. Eidgenössische Materialprüfungs- und Forschungsanstalt (Empa), Abteilung Akustik / Lärmminderung, Dübendorf.

[9] European Union, 2002. *Directive 2002/49/EC of the European Parliament and of the Council of 25 June 2002 Relating to the Assessment and Management of Environmental Noise*. European Union, Bruxelles, Belgium. URL: https://eur-lex.europa.eu/legal-content/EN/TXT/?uri=celex:32002L0049.

[10] European Union, 2015. *COMMISSION DIRECTIVE (EU) 2015/996 of 19 May 2015 establishing common noise assessment methods according to Directive 2002/49/EC of the European Parliament and of the Council*. Official Journal of the European Union. European Union,

[11] European Union, 2018. *Corrigendum to Commission Directive (EU) 2015/996 of 19 may 2015 establishing common noise assessment methods according to Directive 2002/49/EC of the European Parliament and of the Council*. Official Journal of the European Union. European Union,

[12] European Union, 2020. *COMMISSION DELEGATED DIRECTIVE (EU) 2021/1226 of 21 December 2020 amending, for the purposes of adapting to scientific and technical progress, Annex II to Directive 2002/49/EC of the European Parliament and of the Council as regards common noise assessment methods*. Official Journal of the European Union. European Union,

[13] ICAO, 2018. *Recommended Method for Computing Noise Contours Around Airports. Doc 9911. 2nd ed.* International Civil Aviation Organization (ICAO), Montréal, Canada

[14] Isermann, U. und B. Vogelsang, 2010. *AzB and ECAC Doc.29-Two best-practice European aircraft noise prediction models.* Noise Control Engineering Journal **58**, 455-461.

[15] Jäger, D., C. Zellmann, F. Schlatter, und J.M. Wunderli, 2020. *Validation of the sonAIR aircraft noise simulation model.* Noise Mapping.

[16] Krebs, W., R. Bütikofer, S. Plüss, und G. Thomann, 2004. *Sound source data for aircraft noise simulation.* Acta Acustica united with Acustica **90**, 91-100.

[17] Lobsiger, E., 2005. *IMMPAC, ein Verfahren und Programm zur Berechnung und Darstellung von Fluglärmimmissionen. Version 1.0 vom 15. Mai 2005 (internal report)*. Lobsiger Consulting, Bern

[18] Meister, J., S. Schalcher, J.M. Wunderli, D. Jäger, C. Zellmann, und B. Schäffer, 2021. *Comparison of the aircraft noise calculation programs sonAIR, FLULA2 and AEDT with noise measurements of single flights. Paper No. 388.* Aerospace **8**, 16 pp.

[19] SAE, 1986. *Procedure for the Calculation of Airplane Noise in the Vicinity of Airports. Aerospace Information Report SAE AIR 1845*. Society of Automotive Engineers (SAE), Committee A-21 Aircraft Noise, Warrendale, PA.

[20] SAE, 2006. *Method for Predicting Lateral Attenuation of Airplane Noise. Aerospace Information Report SAE AIR 5662*. Society of Automative Engineers (SAE), Committee A-21 Aircraft Noise, Warrendale, PA.

[21] Schäffer, B., S. Plüss, und G. Thomann, 2014. *Estimating the model-specific uncertainty of aircraft noise calculations.* Applied Acoustics **84**, 58-72.

[22] Schäffer, B., R. Bütikofer, S. Plüss, und G. Thomann, 2011. *Aircraft noise: accounting for changes in air traffic with time of day.* Journal of the Acoustical Society of America **129**, 185-199.

[23] Wunderli, J.M., C. Zellmann, M. Köpfli, M. Habermacher, O. Schwab, F. Schlatter, und B. Schäffer, 2018. *sonAIR - a GIS-Integrated Spectral Aircraft Noise Simulation Tool for Single Flight Prediction and Noise Mapping.* Acta Acustica United with Acustica **104**, 440-451.

[24] Zellmann, C., B. Schäffer, J.M. Wunderli, U. Isermann, und C.O. Paschereit, 2017. *Aircraft Noise Emission Model Accounting for Aircraft Flight Parameters.* Journal of Aircraft **55**, 682-695.

8. Annex: $L_{AS,max}$ comparisons

8.1. Comparison of FLULA2 and CNOSSOS with default settings

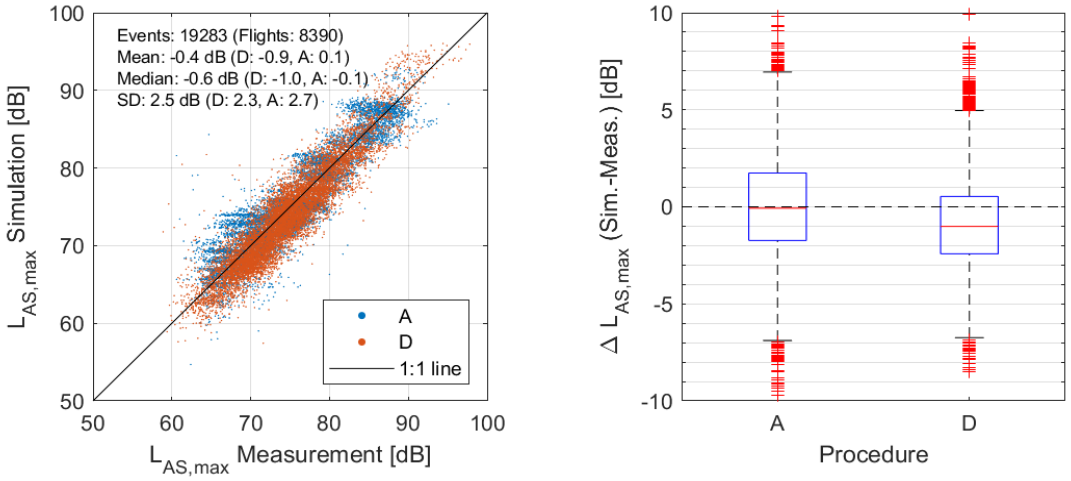

Figure 8-1: **Scatter plot (left) and boxplot (right) of the calculated $L_{AS,max}$ (FLULA2) with the measurements in the vicinity of Zurich and Geneva airports, grouped by departures and approaches.**

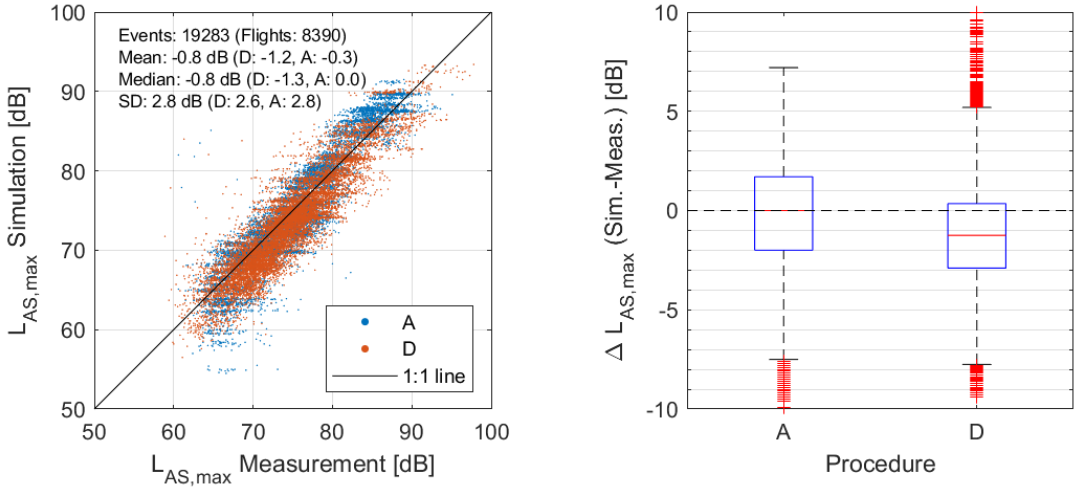

Figure 8-2: **Scatter plot (left) and boxplot (right) of the calculated $L_{AS,max}$ (CNOSSOS) with the measurements in the vicinity of Zurich and Geneva airports, grouped by departures and approaches.**

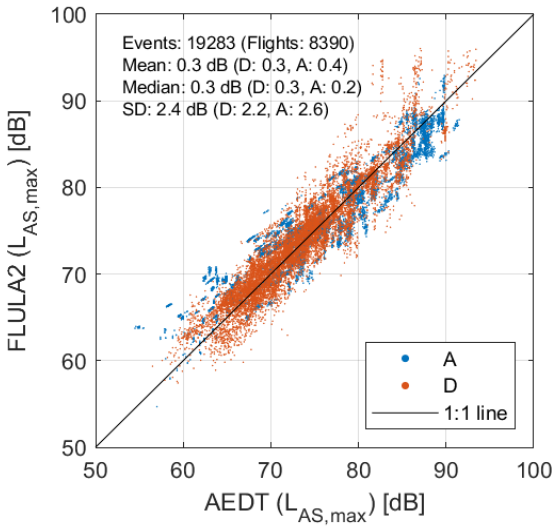

Figure 8-3: **Scatter plot of the calculated $L_{AS,max}$ with FLULA2 with the calculated $L_{AS,max}$ with CNOSSOS in the vicinity of Zurich and Geneva airports, grouped by departures and approaches.**

8.2. Comparison of CNOSSOS with adjusted input data

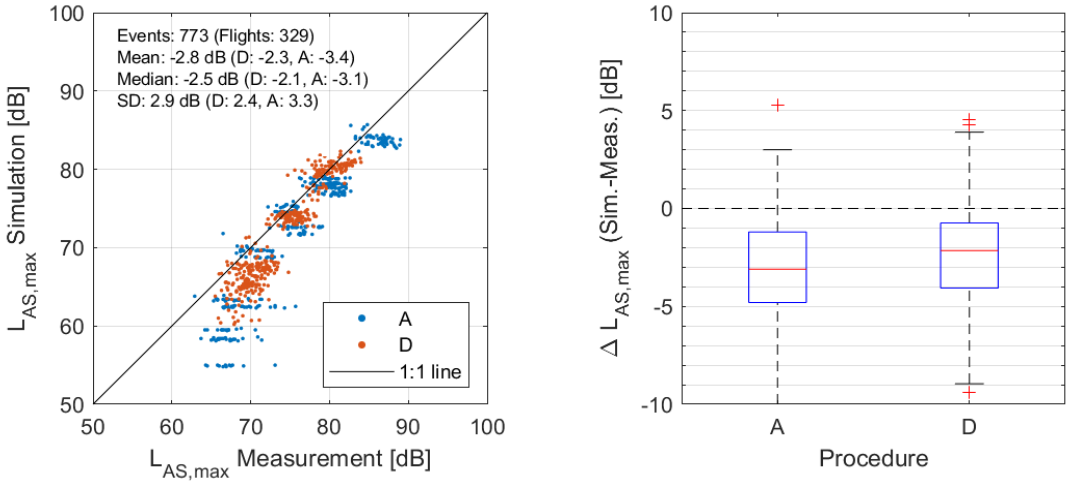

Figure 8-4: **Scatter plot (left) and boxplot (right) of the calculated $L_{AS,max}$ (CNOSSOS) with the measurements in the vicinity of Zurich airports for two narrow-body aircraft types, grouped by departures and approaches.**

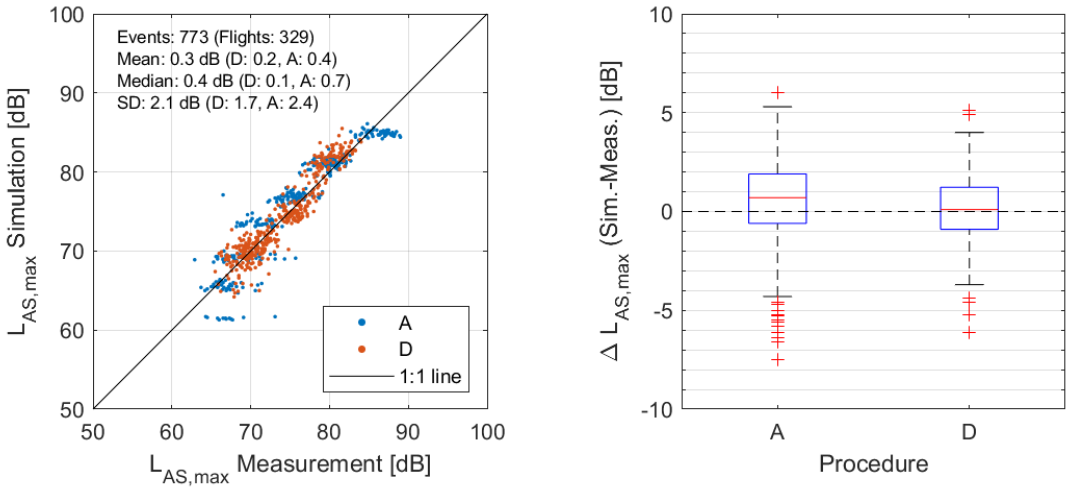

Figure 8-5: **Scatter plot (left) and boxplot (right) of CNOSSOS calculations with adjusted input data: Comparisons of the calculated $L_{AS,max}$ with the measurements in the vicinity of Zurich airports for two narrow-body aircraft types, grouped by departures and approaches.**

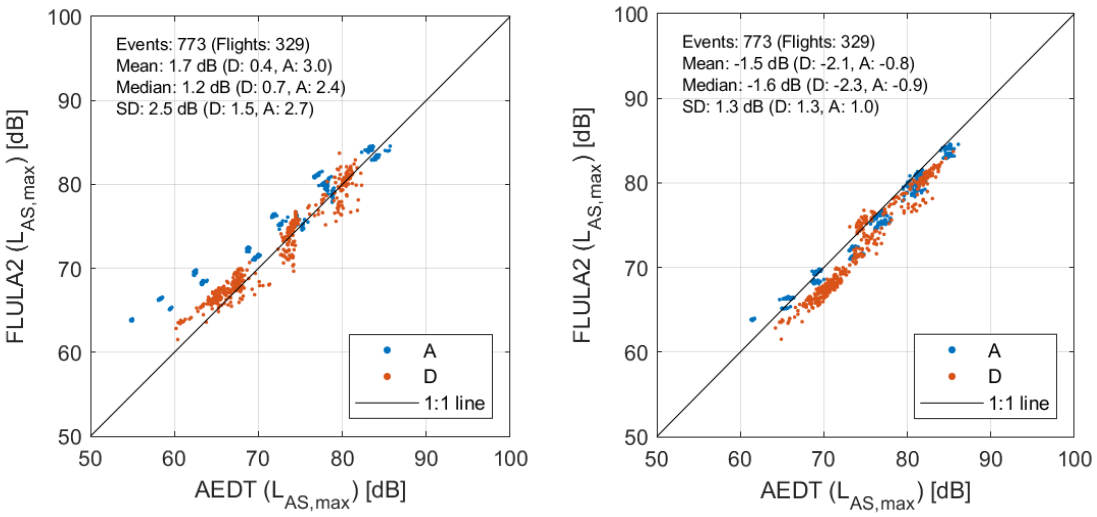

Figure 8-6: **Scatter plots of the calculated $L_{AS,max}$ with FLULA2 in comparison with the simulation with CNOSSOS with default (left) and adjusted (right) input data.**